Moscow University
Physics Bulletin
Vol. 49, No. 4, pp. 81–87, 1994

Vestnik Moskovskogo
Universiteta. Fizika
UDC 621.396

SPECTRAL MODEL OF COHERENT MILLIMETER-BAND SIGNALS REFLECTED FROM VEGETATION

G. I. Khlopov*

Experimental data are presented on the time spectra of coherent signals in the 2 mm band reflected from vegetation at grazing angles. A bicomponent model is proposed for the spectrum of coherent signals reflected from vegetation in the short-wave region of the millimeter band. It is shown that the width of the coherent signal spectrum is much smaller than that predicted by calculations and measurements performed with the aid of incoherent radars.

Much attention is paid to the investigation of the characteristics of coherent signals reflected from vegetation. An important stage of this work is the creation of various models which help to evaluate the reflected signal parameters and, in particular, their spectral characteristics. Such models are widely used for designing methods of suppression of passive interference to ground-based radars, coming from the surface covers, and for remote sensing of the environment. In spite of the great amount of research carried out to date, whose main results are summarized in [1], the data on the millimeter band are very scarce [2–5].

Many experimental data in the long-wave portion of the centimeter band are adequately described by the model [1, 6, 7] according to which the shape of the scattered signal frequency spectrum in its energy-carrying region (down to the level of 10 to 15 dB) can be approximated by a Gaussian curve

$$S(f) = S_0 \exp\{-(f/\Delta f)^2\}, \tag{1}$$

while in the tail regions (below 15 to 20 dB) the spectrum follows a power dependence

$$S(f) = \frac{S_0}{1 + (f/\Delta f)^n}, \tag{2}$$

where Δf is the full spectrum width at half maximum and n is an empirically determined number.

This "piecewise" approximation, however, does not allow one to describe the spectrum shape as a whole and, moreover, it remains unclear how well expressions (1) and (2) describe the spectral characteristics of reflected signals in the millimeter band, especially in its short-wave region.

On the other hand, in practice it is often sufficient to know the integral characteristics of the spectrum, such as its effective width

$$\Delta f_{\text{eff}} = \frac{1}{S_0} \int\limits_0^\infty df\, S(f), \tag{3}$$

where S_0 is the spectral density maximum. In particular, various authors propose the following empirical dependence of the spectrum width of vegetation-reflected signals on the wavelength and the average wind velocity $\overline{v}$ [1, 3, 6, 7]

$$\Delta f_{\text{eff}} = (\beta/\lambda)\overline{v}^{\gamma} \text{ (Hz)}, \tag{4}$$

* Institute of Radiophysics and Electronics, Ukrainian Academy of Sciences, Kharkov.

where the exponent γ is 1 to 1.3, λ is the wavelength (in meters), and the constant β depends on the depth of random modulation of the velocities of individual scatterers b wind waves ($\beta = 2\sqrt{2}m$, where $m = 0.05$ according to [3]). If one substitutes into (4) the available estimates for the appropriate parameters, the resulting width of the passive interference spectrum turns out to be so great that the usefulness of developing complex transmitter/receiver hardware for coherent radars becomes dubious, because the efficiency of such radars would be very low.

Therefore it is crucially important to find out to what extent the mechanisms of reflected signal formation which are characteristic for the long-wave portion of the microwave band remain valid for millimeter-band radio waves, and to what extent the spectrum models developed are applicable in the case of coherent signals.

We performed in situ measurements of the Doppler spectra of 140-GHz signals reflected from tall grass (0.3 to 0.5 m), bush, a solitary tree (birch), and the edge of a deciduous forest, at grazing angles not exceeding 1°. The measurements were performed for a year with the same objects, and the data were grouped in two periods, spring/summer and autumn/winter, corresponding to the presence and absence of the foliage. The wind parameters were monitored with an M-63-1 anemorhumbometer.

Since spectrum evaluation based on finite-length realizations yields statistically inconsistent estimates, various averaging techniques were used. In our studies we used the energy spectrum evaluation method based on Welch periodograms [8].

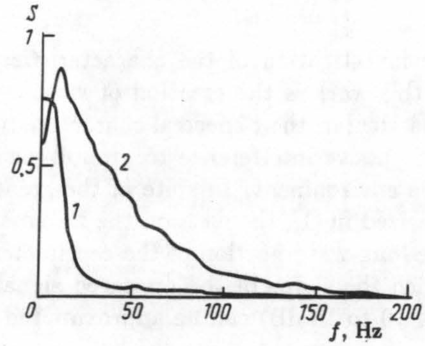

Fig. 1

Spectrum of coherent signals reflected by the grass cover (1) and a solitary tree (2).

It was found that the shapes of the spectrum quite often could not be approximated by expression (1) or (2). For example, a typical spectrum of grass-reflected signals (Fig. 1, curve 1, $\overline{v} = 3$ m/s) is adequately approximated by a Gaussian curve in its energy-carrying portion and by power function (2) at its tail. The presence of a great number of equivalent reflectors, which is typical of a grass cover, favors coincidence of the experimental and approximating functions in the long-wave band portion. For signal reflection by a solitary tree (Fig. 1, curve 2, $\overline{v} = 3.5$ m/s), when both large (trunk, branches) and small (leaves, small branches) reflectors can be discerned, neither approximation (1) nor (2) fits.

The data collected by us suggest the following mechanism of formation of a spectrum of coherent signals reflected by vegetation. Large reflectors (trunk, branches) perform relatively slow oscillations with a high amplitude, which is the reason for a deep phase modulation of the signal. This modulation shifts the spectrum peak frequency by f_0, while rapid displacements of smaller scatterers (leaves, ears, etc.) mainly cause its amplitude fluctuations.

Thus, when building a spectral model for coherent signals reflected from vegetation, including trees, a Doppler frequency shift due to oscillations of large objects must be taken into account. Therefore we propose to describe the spectral density of reflected signals by a bicomponent model

$$S(f) = \frac{S_0}{1+\mu}\left[\frac{f^{2m-1}}{S_g}\exp\left\{-m\left(\frac{f}{\Delta f_D}\right)^2\right\} + \frac{\mu}{1+\left(\frac{f-f_0}{\Delta f_a}\right)^n}\right], \qquad (5)$$

where

$$m = \frac{1}{2}\left[1 - \left(\frac{f_0}{\Delta f_D}\right)^2\right]^{-1},$$

$$S_g = \Delta f_D^{2m-1}\left(\frac{2m-1}{2m}\right)^{\frac{2m-1}{2}} \exp\left\{-\frac{2m-1}{2}\right\}. \qquad (6)$$

The first term corresponds to Nakagami's m-distribution [9], which, in contrast to the Gaussian one, contains bursts which are due to a narrow spectral peak wandering along the frequency axis.

The second term corresponds to power dependence (2), incorporating the shift of the spectrum maximum by f_0 (Fig. 1, curve 2). The parameters of the proposed bicomponent model of the spectrum are the width of the Doppler spectral component Δf_D, the width of the amplitude spectral component Δf_a, the spectrum mode f_0 (the Doppler frequency shift), the decrement of the amplitude component n (the decay rate of the AM component), and the ratio of the amplitude and Doppler spectral component peaks $\mu = S^a_{\max}/S^D_{\max}$.

In the case of small Doppler spectrum shifts ($f_0 \to 0$), this model is transformed into the well-known expressions which describe the scattering of noncoherent signals [1, 3, 6, 7].

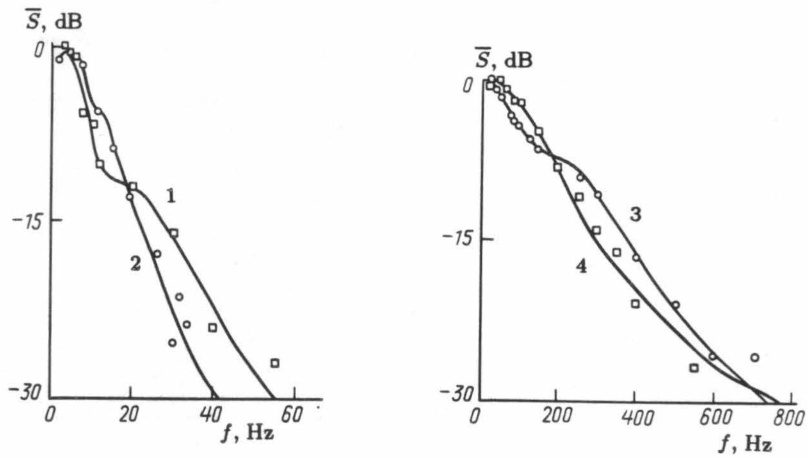

Fig. 2

Normalized experimental spectra of coherent signals reflected from grass (1), forest (2), bush (3), and tree (4) (symbols) in comparison with the mathematical model (solid curves).

The proposed model (5) allows one to control the spectrum shape when approximating experimental data. Figure 2 shows experimental estimates of normalized spectra. One can see that the model (solid curve) fits the experimental data satisfactorily.

We analyzed the experimental data in order to investigate the dependence of the model parameters Δf_D, Δf_a, f_0, μ, n, and S_0 on the wind velocity v for scattering of millimeter-band waves by various types of vegetation. The results are shown by graphs in Figs. 3–5.

The following conclusions can be drawn from this analysis.

1. The width of the Doppler spectral component Δf_D does not exceed tens of hertz (see Figs. 3 a and 4 a) in all cases except reflection from a solitary tree; Δf_D is an order of magnitude smaller than the same parameter for the amplitude spectral component Δf_a (Figs. 3 b and 4 b).

2. The frequency shift of the spectrum maximum f_0 (Figs. 3 c and 4 c) is the highest for solitary-tree reflection.

3. The damping of the amplitude component (Figs. 3 d and 4 d) is the highest for low wind ($n \approx 5$–6) and decreases with growing wind velocity ($n \approx 1$–3).

4. At low wind velocities ($\overline{v} \leqslant 5$–6 m/s) the energy-carrying portion of the spectrum (Figs. 3 e and 4 e) is nearly totally determined by the Doppler component ($\mu \leqslant 0.1$–0.4); with growing wind velocity the

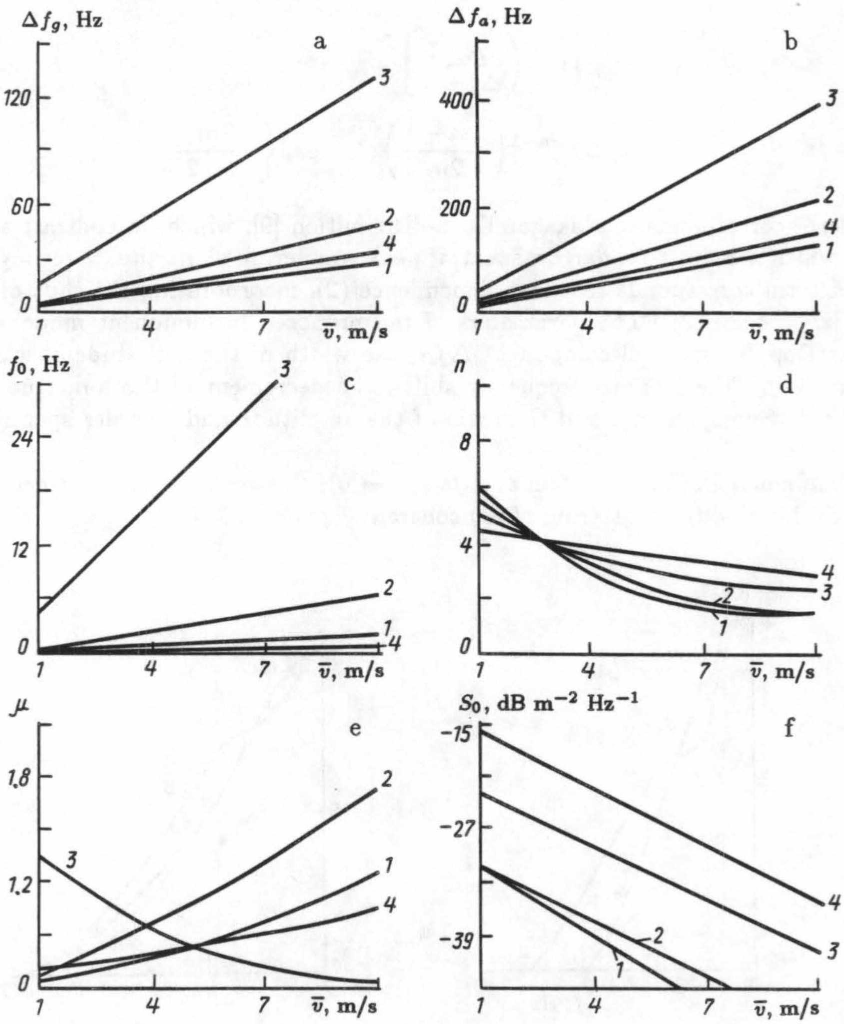

Fig. 3

Parameters of the mathematical model as functions of mean wind velocity: the width of the Doppler component f_D (a), the width of the amplitude component f_a (b), the spectrum mode f_0 (c), the decrement of the amplitude spectrum n (d), the ratio between the amplitude and Doppler components μ (e), and the spectral maximum S_0 (f) for the spring/autumn period. Curves 1 to 4 correspond to grass, bush, tree, and forest, respectively.

contributions from the Doppler and amplitude components become comparable ($\mu \approx 1$), the only exception being the case of solitary-tree reflection.

5. The spectral density maximum S_0 (Figs. 3f and 4f) is inversely proportional to the wind velocity.

Comparison of the data for the spring/summer (see Fig. 3) and autumn/winter (see Fig. 4) periods shows that the absence of foliage cover decreases the numerical values of the above parameters by a factor of 2 or 3, the shapes of the curves remaining the same. Furthermore, if in the spring/summer period the widest spectrum of reflected signals is that for a solitary tree, in the autumn/winter period the solitary-tree and bush reflections are comparable.

The parameter S_0 depends not only on the reflecting properties of the scattering object but also on the bandwidth over which the energy of the fluctuating signal is distributed. Indeed, let us calculate the

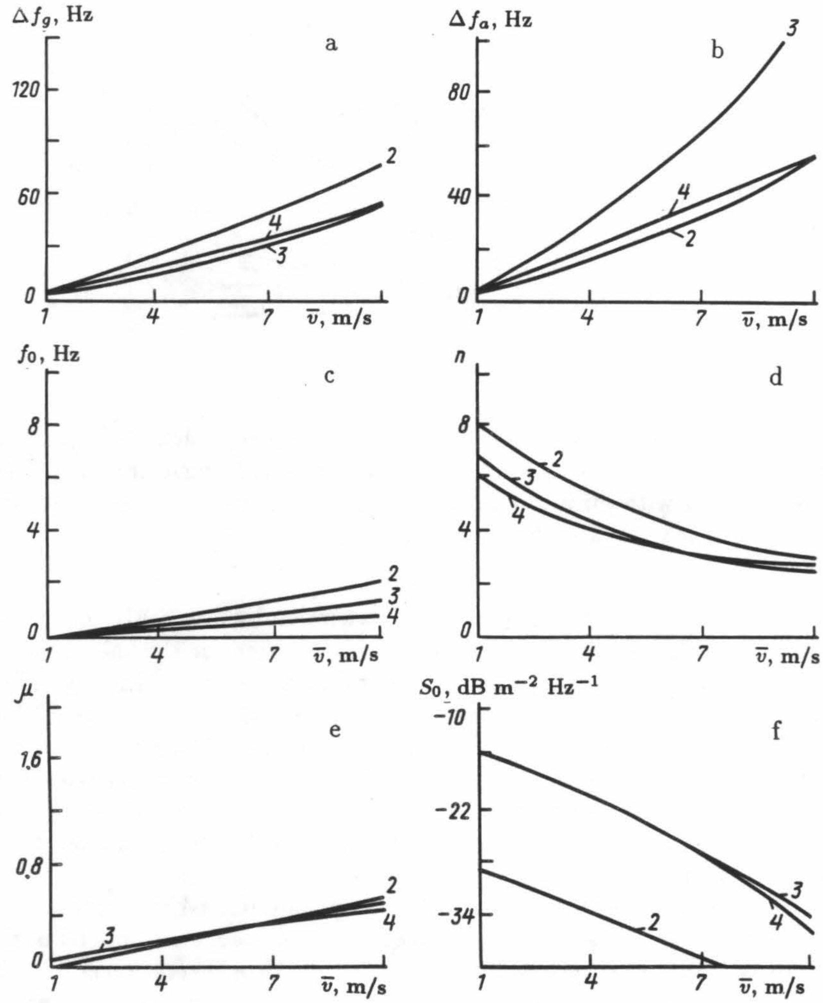

Fig. 4

Parameters of the mathematical model for the autumn/winter period (the notation is the same as in Fig. 3).

effective scattering cross section of the surface cover, measured by a coherent radar:

$$\sigma\ (\mathrm{m}^2) = \Sigma_q \int_{f_f-\Delta f}^{f_f+\Delta f} df\, S(f), \tag{7}$$

where Σ_q is the illuminated surface area (m^2), f_f is the tuning frequency of the Doppler moving-target detection filter, and Δf is that filter's passband. Then the spectral maximum measured by an incoherent radar can be approximately expressed in terms of σ:

$$S_0 \left(\frac{\mathrm{dB}}{\mathrm{m}^2\ \mathrm{Hz}}\right) = \frac{\sigma}{\Delta f_{\mathrm{eff}}}. \tag{8}$$

Comparing formulas (7) and (8), we see that signals that fluctuate in a wide frequency band may provide a spectral-density maximum comparable to that for a relatively narrow-band signal. For instance, the spectra of signals scattered by the bush and grass have S_0 of the same order of magnitude (Fig. 3f), although they

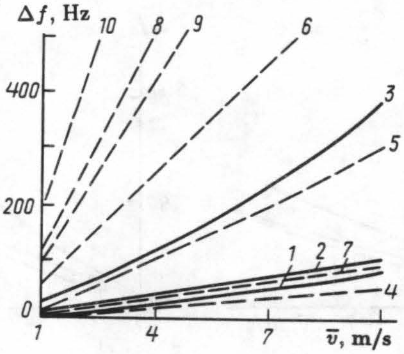

Fig. 5

Effective spectrum width as a function of mean wind velocity calculated according to [1, 3] (curves 5 and 6) or measured with a coherent radar for grass, bush, tree, and forest (curves 1–4, respectively) and with an incoherent radar for grass, tree, and forest (curves 7, 8 for $\lambda = 2.2$ mm, curve 9 for $\lambda = 3.16$ mm, and curve 10).

differ in the integral values of the effective scattering cross section by 5 to 8 dB in the incoherent case [1–4]. The integral effective scattering cross sections are virtually the same for the solitary tree and the forest (if the tree is covered by the antenna beam), but their spectral maxima are noticeably different (see Fig. 3 f).

In order to compare the data of our experiments with those published earlier [1–4], the effective spectrum width (3) was calculated. The calculated data are shown in Fig. 5. Curves 1, 2, 3, and 4 correspond to signals reflected by grass, bush, solitary tree, and forest. Curves 5 and 6 were calculated according to Eq. (4) for the parameters $\gamma = 1.3$, $\beta = 0.032$ and $\gamma = 1$, $\beta = 2\sqrt{2}m$ ($m = 0.05$), following the recommendations given in [1] and [3]. The data calculated by Eq. (4) are significantly different from those obtained on the basis of the two-scale spectrum model (5).

An analysis of the experimental spectra of signals of a millimeter-band coherent radar, scattered by various types of vegetation, showed that a more complete and more adequate model of these spectra can be obtained if one takes into account the scattering not only by a uniform vegetation cover (grass, bush) but also by solitary trees, which is associated with the physical details of scattered signal formation by objects of this type. This conclusion follows from the comparison of curves 1–4 and 7–10 in Fig. 5. These data also show that the spectral width of millimeter-band coherent signals reflected from vegetation is much smaller than the values predicted in [1, 3] and also those produced in experiments carried out with incoherent radars [2–4]. These discrepancies point to different mechanisms of reflected signal formation for coherent and incoherent millimeter-band radars.

Our results show that the proposed bicomponent model can be used to evaluate the level of passive interference due to reflection from vegetation at the input of coherent millimeter-band radars. The model parameters depend on the season and, to a lesser degree, on the wind direction.

REFERENCES

1. G. P. Kulemin and V. B. Razskazovskii, *Scattering of Millimeter Radio Waves by the Earth Surface at Small Angles* (in Russian), Kiev, 1980.
2. G. A. Andreev and A. A. Potapov, *Zarubezhn. Radioelektron.*, no. 11, p. 28, 1984.
3. G. A. Andreev, A. A. Potapov, and G. I. Khokhlov, *Radiotekhn. Elektron.*, vol. 27, no. 10, p. 1863, 1982.
4. R. N. Trebits, R. D. Hages, and L. C. Bomar, *Microwave J.*, vol. 21, no. 8, p. 49, 1978.
5. V. S. Korostelev, G. I. Khlopov, and V. P. Shestopalov, *Izv. Vyssh. Uchebn. Zaved. Radiofiz.*, vol. 33, no. 8, p. 895, 1990.
6. N. A. Armand, V. A. Dyakin, I. N. Kibardina, et al., *Radiotekhn. Elektron.*, vol. 18, no. 7, p. 1337, 1973.

7. V. A. Kapitonov, Yu. V. Melenchuk, and A. A. Chernikov, *Radiotekhn. Electron.*, vol. 18, no. 9, p. 1816, 1973.
8. S. L. Marple, Jr., *Digital Spectral Analysis with Applications,* Prentice Hall, Englewood Cliffs, 1987.
9. M. G. Kendall and A. Stewart, *Theory of Distributions,* Wiley, New York, 1962.